find that several factors contribute to the failure of one RyR channel opening to opens adjacent RyRs as $[Ca]_{SR}$ declines: 1) the lower $[Ca]_{SR}$ reduces driving force and thus limits local $[Ca]_{Cleft}$ (both absolute level and rate of rise), 2) low $[Ca]_{SR}$ can inhibit RyR open time (τ_O) which further reduces local $[Ca]_{Cleft}$ attained, 3) the low τ_O and fast $[Ca]_{Cleft}$ dissipation after closure shorten the opportunity for neighboring RyR activation, 4) at low $[Ca]_{SR}$ the RyR2 exhibits reduced $[Ca]_{Cleft}$ sensitivity. We conclude that all of these factors conspire to reduce the probability of Ca sparks as $[Ca]_{SR}$ declines, despite continued RyR-mediated SR Ca leak.

3030-Pos Board B135

Mitochondrial-SR Ca^{2+} Cycling Modulates Normal Automaticity of Rabbit Cardiac Sinoatrial Nodal Pacemaker Cells

Yael Yaniv, Harold A. Spurgeon, Alexey E. Lyashkov, Bruce D. Ziman, Edward G. Lakatta.

A coupled-clock system within sinoatrial node cells (SANC) confers robustness and regulates their normal automaticity: basal cAMP-mediated, protein kinase A-dependent phosphorylation of Ca^{2+} cycling-proteins enables sarcoplasmic reticulum (SR) to generate spontaneous rhythmic Local, subsarcolemmal Ca^{2+}Releases (LCRs) (''Ca^{2+} clock''). LCRs activate an inward Na^+-Ca^{2+} exchange current that accelerates the diastolic depolarization promoting the ensemble of surface membrane ion channels (''membrane clock'') to generate the next action potential (AP). Intracellular Ca^{2+} enters mitochondria through the mitochondrial uniporter and is extruded by the mitochondrial Na^+-Ca^{2+} exchanger. We hypothesized that mitochondrial Ca^{2+} cycling is coupled to SANC-clocks via its impact on the intracellular Ca^{2+} cycling.

Specific inhibition of Ca influx into and efflux from mitochondria in intact single isolated SANC was effected by Ru360 and CGP-37157, respectively. Changes in mitochondrial Ca^{2+} content (Ca_m) were indexed by selective quenching of the fluorescent Ca^{2+} probe, Indo-1 in the cytosol by Mn^{2+}. Ru360 decreased Ca_m to $80 \pm 8\%$ control and increased the spontaneous SANC AP firing rate to $111 \pm 1\%$. Conversely, CGP-37157 increased Ca_m to $119 \pm 7\%$ control and reduced the spontaneous AP firing rate to $89 \pm 2\%$. Blocking Ca influx into mitochondria increased the average LCR size (measured via confocal linescans images of fluo-4) from 4.2 ± 0.1 to $6.1 \pm 0.2\mu m$ and reduced the normal LCR period from 317 ± 5 to 274 ± 6ms. In contrast, inhibition of Ca efflux from mitochondria reduced LCR size to $3.6 \pm 0.1\mu m$ and increased LCR period to 389 ± 7ms. Changes in LCR period by specific inhibition of Ca^{2+} influx or efflux into and from the mitochondria from 274 ± 6 to 389 ± 7ms predicted (R^2=0.84) the concomitant changes in the spontaneous SANC AP cycle length from 349 ± 5 to 462 ± 6ms.

We conclude that Ca^{2+} cycling into and out of mitochondria interact with the SANC coupled-clock system to modulate normal automaticity.

3031-Pos Board B136

Stochastic Beat-To-Beat Variation in Periodicity of Local Calcium Releases Predicts Intrinsic Cycle Length Variability in Single Sinoatrial Node Cells

Oliver J. Monfredi, Larissa A. Maltseva, Mark R. Boyett, Edward G. Lakatta, Victor A. Maltsev.

Abstract: In sinoatrial nodal cells (SANC), spontaneous, rhythmic, submembrane sarcoplasmic reticulum (SR)-generated local Ca2+ releases (LCRs) that occur during diastolic depolarization (DD) activate inward Na+/Ca2+-exchange currents that accelerate the DD rate. LCRs are roughly periodic, 'LCR period' being the time from the preceding AP-induced Ca2+-transient peak to their subsequent appearance. Previously, we demonstrated that in a given steady-state, the average LCR period of multiple AP cycles predicts concurrent average steady-state AP cycle length. We tested whether variation in LCR periods also predicts the beat-to-beat cycle length within a given steady-state. Methods: We imaged single rabbit SANC using a fast 2D-camera to capture almost all LCRs (in contrast to the relative few LCRs captured by line scan images), and in selected cells we also simultaneously measured APs by perforated patch clamp. Results: LCRs begin to occur very early during diastole, on the descending part of the prior AP-induced Ca2+ transient, shortly after the maximum diastolic potential (MDP). About 40 ms after the MDP, the ensemble of waxing LCR activity causes a late diastolic Ca elevation accompanied by a notable DD acceleration. On average, SANC (n = 9) generated 13.2 ± 3.7 LCRs per cycle, varying in size (7.1 ± 4.2μm) and duration (44.2 ± 27.1 ms). The LCR size and duration were greater for later-occurring LCRs. The average LCR period for a given cycle ranged from 70-460ms, and closely predicted (R2=0.89) the time of occurrence of the next AP, i.e. the duration of that cycle (220 to 470 ms). Numerical modeling simulations closely reproduce this experimental result. Conclusion: Intrinsic cycle length variability in single SANC is linked to cycle to cycle stochastic variations in roughly periodic LCRs.

3032-Pos Board B137

Spatially Complex Diffraction-Limited Photolysis of Caged Calcium and IP3 Combined with High-Speed Confocal Imaging

Vyacheslav M. Shkryl, Joshua T. Maxwell, **Lothar A. Blatter**.

The novel Mosaic digital illumination system (Photonic Instruments/Andor Group) integrated into a Nikon A1R confocal microscope was used to uncage Ca (DM-nitrophen, NP-EGTA) or IP_3 from multiple geometrically complex (Fig.) diffraction-limited subcellular regions and simultaneously measure $[Ca]_i$ with high-speed 2-dimensional confocal imaging (430 fps). The Mosaic System uses a computer controlled spatial light modulator to map a diffraction limited mask onto the specimen plane. A Digital Micromirror Device, consisting of a high speed array of hinge-mounted individually addressable, tiltable microscopic mirrors, directs continuous wave laser light (405 nm) onto the image plane according the user-defined diffraction limited mask. Local uncaging of Ca from multiple small regions of interest (0.63 micrometer diameter) generated artificial Ca sparks outside the cell and produced CICR inside permeabilized cardiac myocytes. Uncaging Ca from a 0.63x10 micrometer region triggered CICR and propagating Ca waves. Subsarcolemmal uncaging of IP_3 initiated propagating Ca waves that originated within the region of uncaging, and caused increased peak amplitude of electrically evoked Ca transients and Ca alternans, suggesting that in cardiac myocytes Ca release from IP_3 recpetors primes ryanodine receptor Ca release channels and enhances CICR.

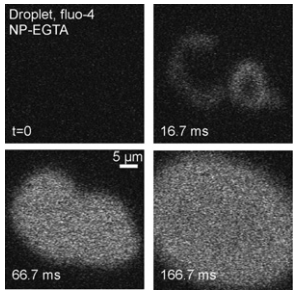

3033-Pos Board B138

Calcium Spark Termination: Ryanodine Receptor Unitary Flux Dependent Mechanism

Tao Guo, Dirk Gillespie, Michael Fill.

Spontaneous sparks seem to terminate at a fixed free sarcoplasmic recticulum Ca concentration ([Ca]SR) indicating that the SR luminal Ca level is a key factor in terminating Ca sparks. In principle, such luminal Ca control could be achieved by different mechanisms. One is that luminal Ca may alter RyR2 gating by acting at intra-SR sites. Another is that, as luminal Ca falls, RyR2 unitary release flux (iCa) may become insufficient to support continued inter-RyR2 Ca-induced Ca release within a RyR2 cluster (a cytosolic process). To date, it has been virtually impossible to experimentally distinguish these possibilities in cells. We have overcome this obstacle by devising a means to manipulate iCa independently of [Ca]SR. This was accomplished by exploiting RyR2 permeation properties. Briefly, sparks and [Ca]SR were simultaneously recorded in permeabilized rat myocytes. Unitary RyR2 iCa in the tested cellular solutions was defined using single RyR2 measurements in bilayers as well as a well-established RyR permeation model. Preliminary data reveal that reducing RyR2 iCa (at a relatively constant [Ca]SR) dramatically decreases spark frequency. We believe this method is the first to experimentally delineate the contribution of RyR2 iCa flux in the SR luminal Ca control of sparks in cardiomyocytes.

3034-Pos Board B139

4-D Scanning of Calcium Sparks in Cardiomyocytes Reveals their In-Focus Amplitude

Vyacheslav M. Shkryl, Lothar A. Blatter, Eduardo Ríos.

Ca sparks, puffs and related discrete events of intracellular Ca release have so far been studied by imaging fluorescence of a suitable monitoring dye over one or two spatial coordinates and time (xt or xyt modes). By missing the vertical (z) coordinate either technique is susceptible to the out-of-focus error. This error corrupts every measurement, especially altering the measurement of amplitude, which is crucial for evaluation of numbers of contributing channels and other features with mechanistic implications. Existing theory of spark scanning (Izu et al.1998; Ríos et al. 2001) allow correction of the out-of-focus error, but only in a statistical sense, leading to correct distributions rather than accurate amplitudes of individual sparks. We now use a fast confocal slit scanner (5-LIVE; Zeiss) to image sparks in x, y and z as they evolve in time, and take advantage of the added dimension to characterize those sparks that are in focus. The distribution of amplitudes of 1196 such sparks (33 cat atrial cells) was not a sum of decaying exponentials, indicating that their Ca sources are non-Markovian channels (in agreement with Ríos et al. 2001, Wang et al. 2002), due for instance to interactions within the cluster. The directly determined distribution of amplitudes was similar to that obtained by correction, according to the theory of spark scanning, of the distribution in a larger sample imaged in xt linescans (xt-to-xyzt correction). The theory is generalized to